FIRST RESULTS ON D DECAYS FROM MARK III*

JAY HAUSER
(Representing the Mark III Collaboration[1])
California Institute of Technology
Pasadena, California 91125

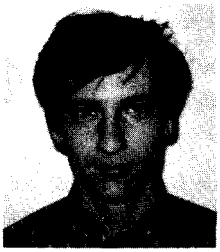

ABSTRACT

We present a preliminary analysis based on 60% of the current Mark III data sample taken at the Ψ''. Several new D decay modes have been found, and several others are confirmed. Dalitz plots of four Cabibbo-favored $K\pi\pi$ decays are presented. We make a qualitative comparison between D^0 decay rates in the Cabibbo-favored $K^-\pi^+$ mode, and in the Cabibbo-suppressed K^+K^- and $\pi^+\pi^-$ modes. Finally, we discuss the future prospects for D meson analysis by Mark III.

* Work supported by the Department of Energy, contract DE-AC03-81ER40050.

1. Introduction

The discovery of the Ψ'' has made available new opportunities for studying the decays of charmed particles. The width of the resonance is more than two orders of magnitude larger than the widths of the Ψ and Ψ', because its mass lies above the threshold for decays to openly charmed particles. In fact, the Ψ'' is not massive enough to decay into $D\bar{D}^*$, but decays almost 100% to $D\bar{D}$ pairs. For an e^+e^- experiment, this gives running at the center-of-mass energy of the Ψ'' several advantages:

1. A large $D\bar{D}$ production cross-section of 8 nb, or about one-fourth of all hadronic events.
2. The D's are produced at a fixed momentum, providing an important means of isolating D signals from background.
3. The momenta of final-state particles from D decays are low, allowing effective particle identification by time-of-flight and dE/dX measurement.

At this time, Mark III has accumulated a total of $\sim$ 9000 nb^{-1} of data at the Ψ'', of which $\sim$ 5000 nb^{-1} was used in this analysis. Results presented are preliminary, and primarily qualitative in nature.

The study of D decays focuses on two questions; the elements of the weak quark mixing matrix, and the mechanism of weak hadronic decays of heavy mesons.

2. Weak Mixing Matrix

The elements of the weak quark mixing matrix relevant to charm decay are V_{cd} and V_{cs}.[2] The ratio of these matrix elements can be measured unambiguously in the semileptonic decays of D's:

$$\frac{BR(D^0 \to \pi^- e^+ \nu_e)}{BR(D^0 \to K^- e^+ \nu_e)} = \frac{BR(D^+ \to \pi^0 e^+ \nu_e)}{BR(D^+ \to \bar{K}^0 e^+ \nu_e)} = \left|\frac{V_{cd}}{V_{cs}}\right|^2$$

up to phase space and form-factor corrections. The Cabibbo-suppressed semileptonic modes are very difficult to measure however, because of the missing neutrino, and because of their small branching ratios. It may be possible for the Mark III to measure these matrix elements using hadronic D decays, by measuring ratios such as:

$$\frac{BR(D^+ \to \pi^0 \pi^+)}{BR(D^+ \to \bar{K}^0 \pi^+)} = \frac{1}{2} \times \left|\frac{V_{cd}}{V_{cs}}\right|^2$$

The final states in both numerator and denominator are exotic I=2 and I=3/2 states, presumably free of final-state interactions.

Another interesting prediction for hadronic final states relies on SU(3) flavor symmetry and the relation:

$$V_{cd}V_{cs} + V_{ud}V_{us} \approx 0$$

. This approximation is valid in the Kobayashi-Maskawa framework if the B lifetime is as long as has been reported.[3] One can then derive the relation among Cabibbo-suppressed decays:

$$\frac{BR(D^0 \to K^+K^-)}{BR(D^0 \to K^-\pi^+)} = \frac{BR(D^0 \to \pi^+\pi^-)}{BR(D^0 \to K^-\pi^+)} = \left|\frac{V_{cd}}{V_{cs}}\right|^2$$

Data from Mark II appeared to be inconsistent with this relation.[4] We present a comparison of these modes with higher statistics in section 8.

3. The Mechanism of Hadronic Charm Decay

Based on the mass of the charmed quark, it was first thought that QCD calculations within the Light Quark Spectator model [Figure 1(a)] might be able to predict the pattern of charmed meson decays.[5] In particular, this model predicts equal D^+ and D^0 lifetimes. Current experimental evidence suggests that the D^+ lifetime is significantly longer than that of the D^0. Several models have been proposed to explain this.

The Sextet Dominance[6] model basically states that the piece of the charm-changing Hamiltonian which transforms as a sextet under SU(3) dominates that piece which transforms as a 15-plet. The justification for this assumption is that its analogue in strangeness-changing non-leptonic decays predicts the familiar $\Delta I = 1/2$ rule.

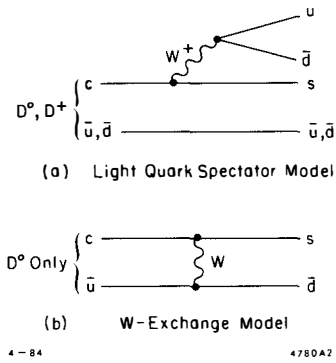

Fig. 1. Diagrams for
(a) the Light Quark Spectator model,
and (b) the W-Exchange model.

The W-exchange[7] model states that the diagram of Figure 1(b), which doesn't exist for D^+ decays, plays a significant role in D^0 decays. In this model gluons are needed either explicitly in the final state, or as a component in the D^0 wavefunction, to remove the helicity suppression at the light quark vertex.

Detailed predictions of each of these models appear to disagree with the data. For instance, the Light Quark Spectator model predicts suppression of D^0 decays to $\bar{K}^0\pi^0$ by a factor of 18 or more relative to $K^-\pi^+$, whereas the measured ratio is 0.7 ± 0.4.[4] Sextet Dominance predicts that the decay $D^+ \to \bar{K}^0\pi^+$ should be highly suppressed, whereas the measured branching ratio of $(1.8 \pm 0.5)\%$ is not particularly small. The W-exchange model predicts a D^0 final state which is completely I=1/2, so that the ratio of D^0 decays to $\bar{K}^0\rho^0$ versus $K^-\rho^+$ should be 1/2, whereas the data favor a much smaller ratio.[4] It is clear, however, that the experimental numbers need to be improved in order to clarify these discrepancies.

4. Detector

The Mark III detector,[8] shown in Figure 2, was designed specifically to reconstruct exclusive final states in e^+e^- annihilation at center-of-mass energies between three and eight GeV. It has particular advantages over earlier magnetic detectors at SPEAR in solid angle coverage and photon efficiency. The main features of the Mark III detector which were used in this analysis were:

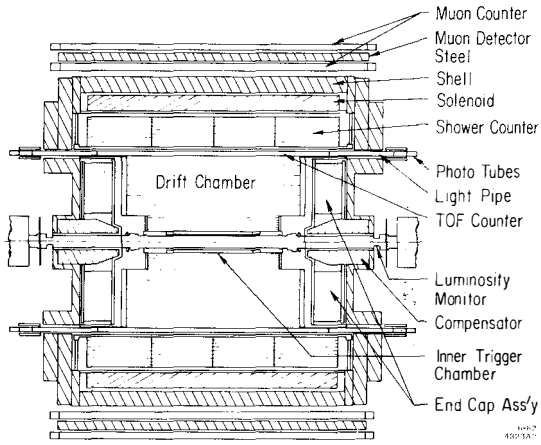

Fig. 2. Side view of the Mark III detector.

1. Solid angle coverage of 95% of 4π for photons, and approximately 93% of 4π for charged tracks.
2. Charged particle momentum resolution of 1.5-2.5% over the relevant momentum range, dominated by multiple Coulomb scattering.
3. High photon efficiency down to 50 MeV with energy resolution given by the equation:

$$\Delta E = 18\% \times \sqrt{E} \text{ where } E \text{ is in GeV}$$

4. Particle identification by time-of-flight (TOF) over 80% of 4π solid angle, with time resolution of 190 ps for hadrons.

5. Known D Decay Modes

We first present our signals in six all-charged D decay modes which have been previously observed. Identification of these modes is made through the following procedure:

1. TOF identification is required for charged kaons.
2. Charged particles which are not identified by TOF are called pions.
3. K^0 decays are identified in the mode $K^0_s \to \pi^+\pi^-$. Loose cuts are imposed on the K^0_s vertex displacement from the interaction region, and on the $\pi^+\pi^-$ invariant mass.
4. All combinations of a desired final state are made. We then form the quantities invariant mass, and beam-constrained mass, defined as:

$$M_{BC} = \sqrt{(E_{beam})^2 - (\sum \vec{P}_i)^2}$$

   These should be equal to the D mass for final states resulting from D decays.
5. A cut of $\pm 2.5\sigma$ is imposed around the D invariant mass, and the beam-constrained mass is plotted.

The resulting beam-constrained mass plots for the D decay modes $K^-\pi^+$, $K^-\pi^+\pi^+$, $K^-\pi^+\pi^+\pi^-$, and $\bar{K}^0\pi^+$, $\bar{K}^0\pi^+\pi^-$, $\bar{K}^0\pi^+\pi^+\pi^-$ are shown in Figure 3. The size of these signals are between two and five times larger than in any previous experiment. Table I compares the number of signal events with the numbers reported by Mark II[4] from SPEAR. In all modes, there is agreement within the statistical errors.

Table I - Comparison of Production of D Decays at the Ψ''

Mode	#Mk II	ϵ(Mk II)	ϵ(Mk III)*	# Expected*	# Seen*
$K^-\pi^+$	263 ± 17	0.39	0.48	511 ± 33	523
$K^-\pi^+\pi^+$	239 ± 17	0.22	0.41	704 ± 50	666
$K^-\pi^+\pi^+\pi^-$	185 ± 18	0.095	0.23	708 ± 69	602
$\bar{K}^0\pi^+$	36 ± 7	0.09	0.16	99 ± 19	69
$\bar{K}^0\pi^+\pi^-$	32 ± 8	0.04	0.10	124 ± 31	163
$\bar{K}^0\pi^+\pi^+\pi^-$	21 ± 9	0.04	0.09	203 ± 68	97

* Preliminary

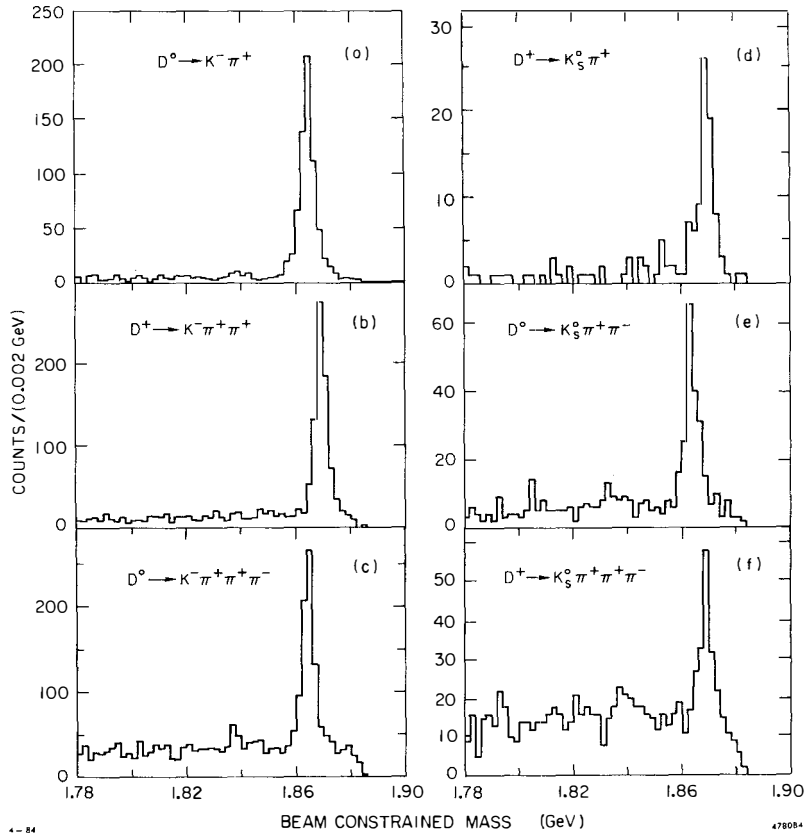

Fig. 3. Mass plots for (a) $K^-\pi^+$, (b) $K^-\pi^+\pi^+$, (c) $K^-\pi^+\pi^+\pi^-$, (d) $K^0_S\pi^+$, (e) $K^0_S\pi^+\pi^-$, and (f) $K^0_S\pi^+\pi^+\pi^-$.

6. Evidence for New Decay Modes

We present two D meson decay modes which were previously reported with marginal statistics, and three decay modes which have not been reported. Several of these are modes with a single π^0, which are analyzed slightly differently than the all-charged decay modes. In these modes, the energies of the two photons from the π^0 decay are refit, because of the poor shower counter energy resolution, according to the two constraints:

$$E_{\gamma 1} + E_{\gamma 2} + E_{chg} = E_{beam}$$

$$2E_1E_2(1 - cos\theta_{12}) = m^2_{\pi^0}$$

The invariant mass is then plotted after a cut of $\chi^2 < 6$ from the 2C fit to the photon energies.

Figure 4 shows signals in the modes $D^0 \to \bar{K}^0\pi^0$ and $D^+ \to \bar{K}^0\pi^+\pi^0$ which were previously reported [4] with 8 ± 4 and 9 ± 5 events, respectively. These signals contain 25 and 105 signal events, confirming these decays with much higher statistics. Figure 5 shows signals in the previously-unseen modes $D^+ \to K^-\pi^+\pi^+\pi^0$ and $D^0 \to \bar{K}^0\pi^+\pi^+\pi^-\pi^-$. The two modes show 65 and 14 signal events respectively.

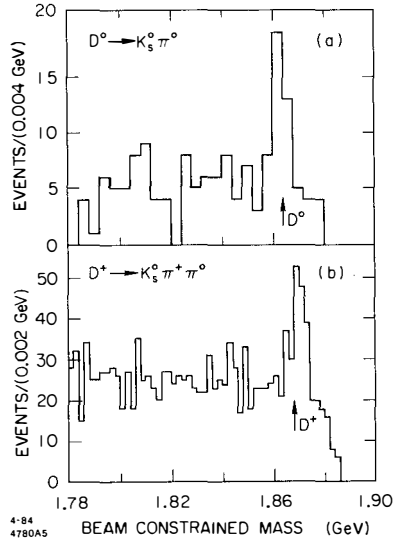

Fig. 4. Mass plots for (a) $K^0_s\pi^0$, and (b) $K^0_s\pi^+\pi^0$.

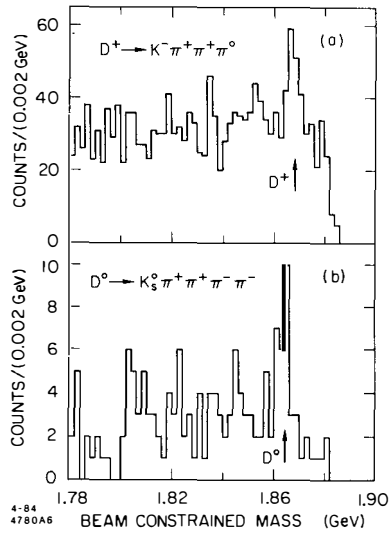

Fig. 5. Mass plots for (a) $K^-\pi^+\pi^+\pi^0$, and (b) $K^0\pi^+\pi^+\pi^-\pi^-$.

Figure 6 shows a very clean signal of 11 events in the mode $D^0 \to \bar{K}^0 K^+ K^-$. Our efficiency is only a few percent for this mode because of decays of the slow kaons, so that this signal actually represents a fairly significant branching ratio. This final state is of particular interest[9] if it arises through the decay sequence

$$D^0 \to \bar{K}^0 \phi^0; \quad \phi^0 \to K^+ K^-$$

This particular decay is not allowed to occur via the Light Quark Spectator model, as the state $\bar{K}^0 \phi^0$ includes no u quark content, whereas the D^0 wavefunction does. The u quark of the D^0 must therefore participate in the diagram, as in the W-exchange model. Figure 7 shows the K^+K^- invariant mass^2 plotted against the $\bar{K}^0 K^+ K^-$ invariant mass, after a ± 50 MeV cut around the D^0 momentum has been applied. It is clear that events cluster at low K^+K^- invariant mass only at the total invariant mass of the D^0, while the phase space distribution peaks at higher K^+K^- mass. However, the width of the K^+K^- mass^2 distribution appears inconsistent with the $\bar{K}^0 \phi^0$ hypothesis, given our detector resolution. Additional data and analysis should help to clarify this situation.

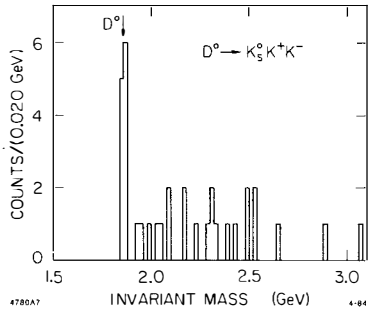

Fig. 6. Mass plot for $K^0_s K^+ K^-$.

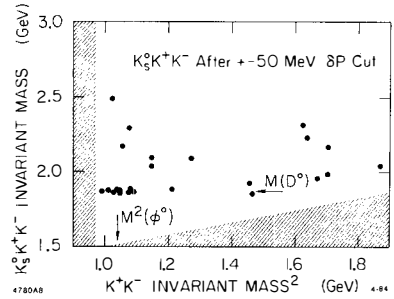

Fig. 7. Plot of K^+K^- mass^2 versus $K^0_s K^+ K^-$ invariant mass after a cut of ± 50 MeV around the D^0 momentum.

7. $D \to K\pi\pi$ Dalitz Plots

The ratios between the various D meson decay amplitudes to pseudoscalar-vector $K\rho$ and $K^*\pi$ final states are determined by the isospin content of the hadronic final state. Knowledge of this content may help to distinguish between different models of hadronic D decays. In addition, the following triangle relationships between the D decay amplitudes can put constraints on the D lifetime measurements, as they relate amplitudes for both D^0 and D^+ decays.

$$A(D^0 \to K^- \rho^+) + \sqrt{2}\, A(D^0 \to \bar{K}^0 \rho^0) - A(D^+ \to \bar{K}^0 \rho^+) = 0$$

$$A(D^0 \to K^{*-} \pi^+) + \sqrt{2}\, A(D^0 \to \bar{K}^{*0} \pi^0) - A(D^+ \to \bar{K}^{*0} \pi^+) = 0$$

Note in particular that if one of the D^0 decay amplitudes vanishes, it leads to an equality between a D^0 decay amplitude and a D^+ decay amplitude. In this case, a measurement of the branching ratios translates into an effective measurement of the D^+ to D^0 lifetime ratio.

Table II contains the list of possible Cabibbo-favored $K\rho$ and $K^*\pi$ decays.

Table II - Cabibbo-allowed $K\pi\pi$ D Decays

Resonance	Final States
$K^-\rho^+$	$K^-\pi^+\pi^0$
$\bar{K}^0\rho^0$	$\bar{K}^0\pi^+\pi^-$
$\bar{K}^0\rho^+$	$\bar{K}^0\pi^+\pi^0$
$K^{*-}\pi^+$	$\bar{K}^0\pi^+\pi^-$ $K^-\pi^+\pi^0$
$\bar{K}^{*0}\pi^+$	$K^-\pi^+\pi^+$ $\bar{K}^0\pi^+\pi^0$
$\bar{K}^{*0}\pi^0$	$K^-\pi^+\pi^0$ $\bar{K}^0\pi^0\pi^0$

We can observe all of these resonances, although the $D^0 \to \bar{K}^{*0}\pi^0$ decay is only visible in the final state $K^-\pi^+\pi^0$. Thus, for the first time, measurements of all three pseudoscalar-vector decays in each triangle relation can be made.

Figure 8 shows the signal in $K^-\pi^+\pi^+$. A cut of ± 5 MeV around the D^+ mass furnishes a sample of some 720 events over a background of 75 events. Figure 9(a) shows the resulting Dalitz plot, with $m^2_{K^-\pi_1^+}$ plotted against $m^2_{K^-\pi_2^+}$. Some part of the decay seems to be associated with $\bar{K}^{*0}\pi^+$, as seen in the projection of Figure 9(b) at $m^2_{K^*}$.

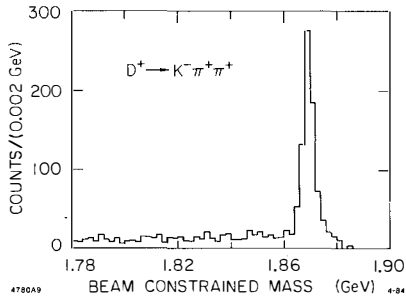

Fig. 8. $D^+ \to K^-\pi^+\pi^+$ signal.

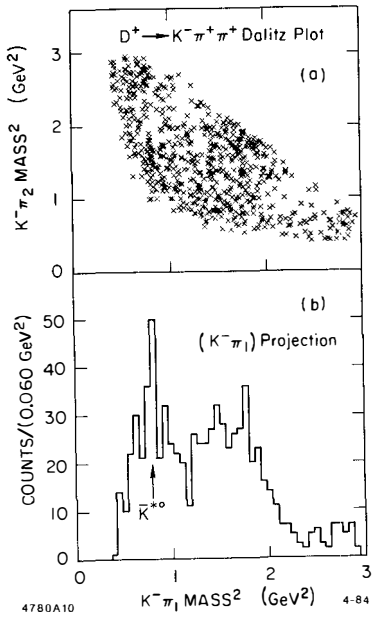

Fig. 9. (a) Dalitz plot for $D^+ \to K^-\pi^+\pi^+$, and (b) $K^-\pi^+$ projection.

Figure 10 shows the signal in $K^-\pi^+\pi^0$. A cut of ± 5 MeV around the D^0 mass furnishes a sample of some 480 events over a background of 400 events. Figure 11(a) shows the resulting Dalitz plot, with $m^2_{\pi^+\pi^0}$ plotted against $m^2_{K^-\pi^+}$. The Dalitz plot shows a strong $K^-\rho^+$ component, as shown in the projection in Figure 11(b). There is some evidence for $\bar{K}^{*0}\pi^0$ and $K^{*-}\pi^+$ production as well. Because of the L=1 decay of the ρ^+, the angular distribution of the pions has a $\cos^2\theta$ distribution relative to the recoiling kaon. This means that the $K^-\pi^+$ mass distribution within the ρ

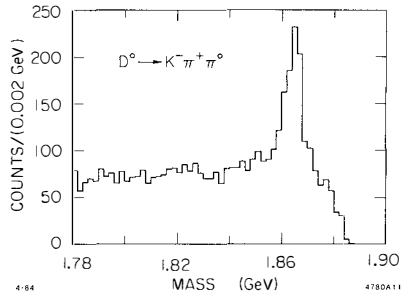

Fig. 10. $D^0 \to K^-\pi^+\pi^0$ signal.

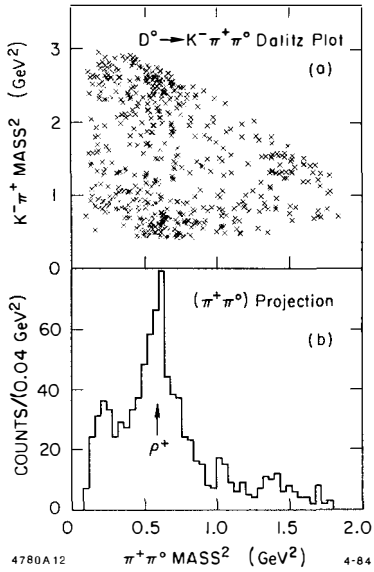

Fig. 11. (a) Dalitz plot for $D^0 \to K^-\pi^+\pi^0$, and (b) $\pi^+\pi^0$ projection.

signal peaks both at high and low mass^2, as can be seen in the Dalitz plot. This is a characteristic of all pseudoscalar-vector decays of D mesons.

Figure 12 shows the signal in $\bar{K}^0\pi^+\pi^-$. A cut of ± 5 MeV around the D^0 mass furnishes a sample of some 153 events over a background of 25 events. The Dalitz plot is shown in Figure 13(a) with $m^2_{K^0\pi_1}$ plotted against $m^2_{K^0\pi_2}$. There are strong signals in K^{*-} and its charge conjugate to be seen in both horizontal and vertical bands at $m^2_{K^*}$. Another choice of axes is shown in Figure

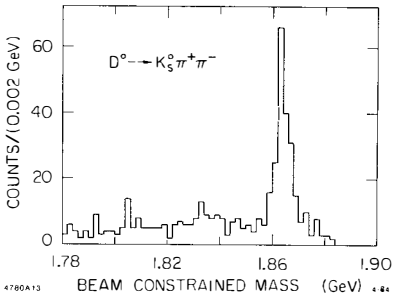

Fig. 12. $D^0 \to K^0_s\pi^+\pi^-$ signal.

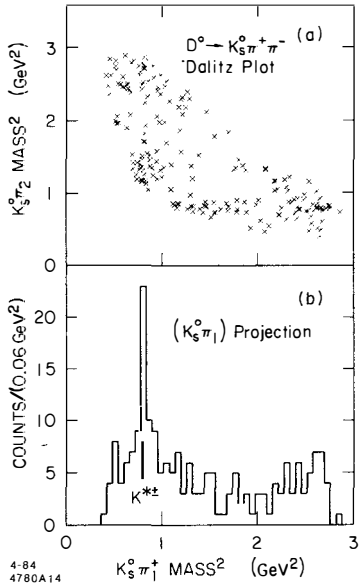

Fig. 13. (a) Dalitz plot for $D^0 \to K^0_s\pi^+\pi^-$, and (b) $K^0_s\pi$ projection.

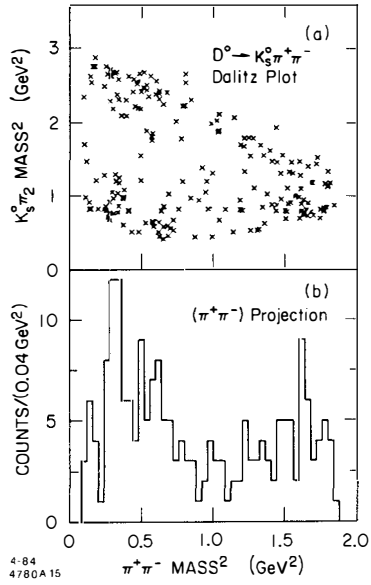

Fig. 14. (a) Dalitz plot for $D^0 \to K^0_s\pi^+\pi^-$, and (b) $\pi^+\pi^-$ projection.

14(a), with $m^2_{\pi^+\pi^-}$ plotted against $m^2_{K^0\pi_1}$. The Dalitz plot and the $\pi^+\pi^-$ projection below in Figure 14(b) show that the amount of $\bar{K}^0\rho^0$ decay appears to be rather small.

The final $K\pi\pi$ Dalitz plot comes from the $\bar{K}^0\pi^+\pi^0$ signal shown in Figure 15, which has 92 signal events over a background of 115 events in the ± 5 MeV signal region. Figure 16(a) plots $m^2_{\pi^+\pi^0}$ against $m^2_{\bar{K}^0\pi^+}$ within the $\bar{K}^0\pi^+\pi^0$ signal. It appears that there is some $\bar{K}^0\rho^+$ component in this decay.

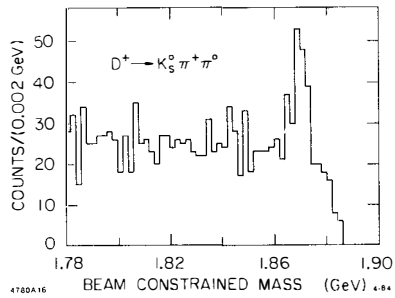

Fig. 15. $D^+ \to K^0_s\pi^+\pi^0$ signal.

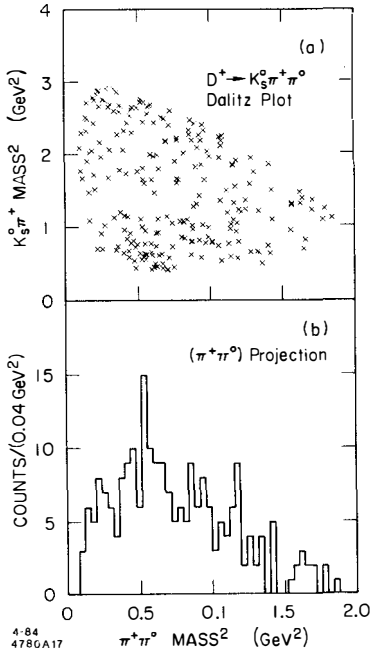

Fig. 16. (a) Dalitz plot for $D^+ \to K^0_S\pi^+\pi^0$, and (b) $\pi^+\pi^0$ projection.

8. Comparison of D^0 Decay to $K^-\pi^+$ Relative to K^+K^- and $\pi^+\pi^-$

The Cabibbo-allowed decay of the D^0 to $K^-\pi^+$ is very similar experimentally to its Cabibbo-suppressed decays into K^+K^- and $\pi^+\pi^-$. The efficiency for the K^+K^- and $\pi^+\pi^-$ modes differ by less than 20 % from the $K^-\pi^+$ mode. Figure 17 shows the signals in these three modes, made with identical cuts except for the TOF classification. The horizontal axis plots invariant mass. The vertical axis plots the difference between the observed momentum and the expected D momentum. The $K^-\pi^+$ plot shows a large signal at the D^0 mass and the correct momentum. The K^+K^- plot shows a smaller peak at the D mass and momentum, and another peak at the correct momentum, but with mass at 1.985 GeV. This peak arises from $K^-\pi^+$ events where the pion has been misidentified by the TOF as a kaon, which increases the invariant mass. Likewise, in the $\pi^+\pi^-$ plot, there is a misidentification peak at 1.740 GeV arising from $K^-\pi^+$ events where the kaon has been misidentified as a pion. The $\pi^+\pi^-$ plot shows only a small enhancement in the D^0 mass region.

The projections in invariant mass are plotted in Figure 18 for these signals after a cut of $\pm$ 40 MeV/c has been applied around the D^0 momentum. The $K^-\pi^+$ plot was fit to a gaussian

plus a quadratic background term. The fit number of events is 453±25 with a sigma of 19 MeV. Then the K^+K^- and $\pi^+\pi^-$ plots were fit to a gaussian with mean fixed at 1.864 GeV and sigma fixed at 19 MeV, plus a gaussian centered on the misidentification peaks with 21 MeV sigma (folding in a smearing due to the Lorentz boost of the D^0), plus a linear background term. The fitted number of events were 52 ± 8 in the K^+K^- mode, and 14 ± 5 in the $\pi^+\pi^-$ mode.

These results appear consistent with the Mark II measurements, and provide further evidence that the D^0 decay to K^+K^- is preferred relative to $\pi^+\pi^-$. Measurements of other Cabibbo-suppressed modes such as $\pi^+\pi^0$ may help to separate SU(3) breaking effects from those due to the mixing matrix.

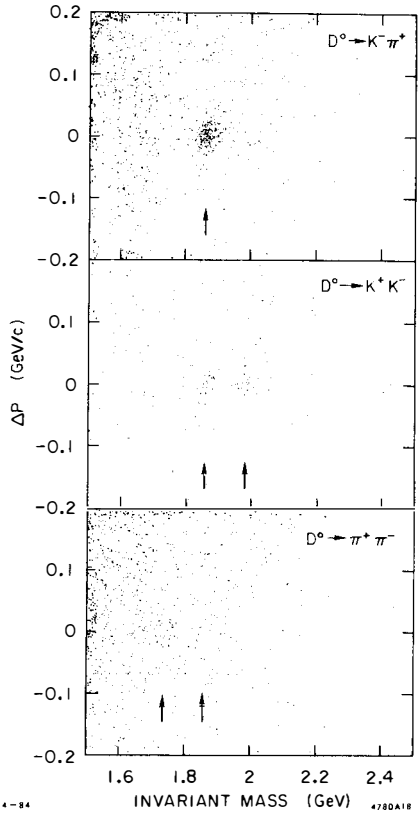

Fig. 17. Plot of invariant mass against deviation from expected D^0 momentum for (a) $K^-\pi^+$, (b) K^+K^-, and (c)$\pi^+\pi^-$.

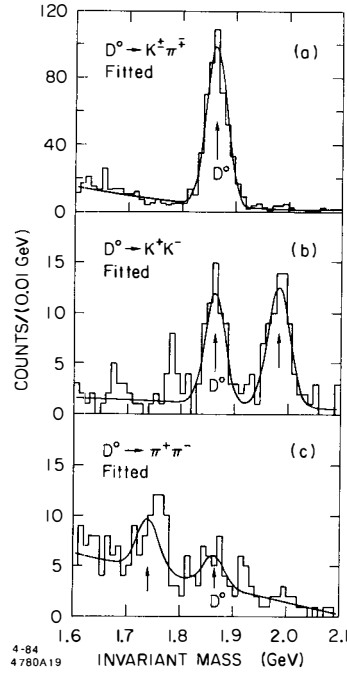

Fig. 18. Invariant mass projections and fits for (a) $K^-\pi^+$, (b) K^+K^-, and (c) $\pi^+\pi^-$.

9. Future Prospects for D Analysis By Mark III

At present, the sum of published branching ratios of D mesons to exclusive final states is 23% for the D^0 and 28% for the D^+. We naturally wish to fill out the list of various D decays. In particular, measurements of the two-body and quasi-two-body decays in pseudoscalar-pseudoscalar, pseudoscalar-vector, and vector-vector modes are to be compared with isospin and SU(3) predictions of various D decay models. We also are looking for decays involving η, η', ω, and ϕ which may serve to distinguish between the D decay models.

Measurements of D branching ratios have always been tied to knowledge of their production rate. At the Ψ'', one assumes that all decays are to $D\bar{D}$ pairs, with the ratio of charged to neutral pairs determined by the D masses. The branching ratios are thereby dependent on several assumptions, and to the shape of R in the region of the Ψ''. With our large data sample, we intend to determine absolute branching ratios by an independent technique, completely free of these assumptions. The branching ratio to a particular large decay mode can be determined by the ratio of $D\bar{D}$ events having both sides reconstructed in that mode, to the number of events having only one D reconstructed in that mode, given enough data. In fact, one can sum several decay modes together, and perform the same analysis. The absolute branching ratio and the production cross-section in that mode or modes then determine the original number of D's produced. We expect to be able to normalize our cross-sections to an accuracy of about 10% by this technique.

Semileptonic decays of D mesons are most easily studied in the recoil from a fully reconstructed D of known strangeness. Since the amplitudes for D^+ and D^0 semileptonic decays are equal, the ratio of the D^+ and D^0 semileptonic branching ratios is equal to the ratio of their lifetimes. Our ability to separate electrons from pions is crucial to this analysis. The misclassification of pions as electrons has been measured as 3% using a combination of TOF and shower counter techniques. There is an additional separation of 3σ using the independent measurement of dE/dX loss in the second layer of our drift chamber. We believe the combination of these techniques should give a reliable measurement of the electron content recoiling from reconstructed D decays, and thus lead to a measurement of the D lifetime ratio to an accuracy of about 20% .

In conclusion, we expect Mark III to make substantial progress toward understanding D meson decays in the very near future.

REFERENCES

1] Members of the Mark III Collaboration are R. M. Baltrusaitis, D. Coffman, G. Dubois, J. Hauser, D. G. Hitlin, J. D. Richman, J. J. Russell, and R. H. Schindler, *California Institute of Technology*; K. O. Bunnell, R. E. Cassell, D. H. Coward, S. Dado, K. F. Einsweiler, L. Moss, R. F. Mozley, A. Odian, J. R. Roehrig, W. Toki, F. Villa, N.

Wermes, and D. E. Wisinski, *Stanford Linear Accelerator Center*; D. E. Dorfan, R. Fabrizio, F. Grancagnolo, R. P. Hamilton, C. A. Heusch, L. Koepke, W. Lockman, R. Partridge, J. Perrier, H. F. Sadrozinski, T. L. Schalk, A. Seiden, and A. Weinstein, *University of California at Santa Cruz*; J. J. Becker, G. T. Blaylock, B. Eisenstein, G. Gladding, S. A. Plaetzer, A. L. Spadafora, J. J. Thaler, B. Tripsas, A. Wattenberg, and W. J. Wisniewski, *University of Illinois, Champaign-Urbana*; J. S. Brown, T. H. Burnett, V. Cook, C. Del Papa, A. L. Duncan, P. M. Mockett, A. Nappi, J. C. Sleeman, and H. J. Willutzki, *University of Washington, Seattle.*

2] L.-L. Chau, Phys. Rep. 95, 1 (1983).

3] E. Fernandez *et al.*, Phys. Rev. Lett. 51, 1022 (1983).

4] R. H. Schindler *et al.*, Phys. Rev. D 24, 78 (1981).

5] J. Ellis, M. K. Gaillard and D. V. Nanopoulos, Nucl. Phys. B100, 313 (1975).

6] B. Guberina, S. Nussinov, R. D. Peccei and R. Rückl, Phys. Lett. 89B, 111 (1979).

7] S. P. Rosen, Phys. Rev. Lett. 44, 4 (1980).

8] D. Bernstein *et al.*, SLAC Report No. SLAC-PUB-3222, 1983 (to be published in Nucl. Instrum. Methods).

9] I. I. Y. Bigi and M. Fukugita, Phys. Lett. 91B, 121 (1980).